

## VELOCITY AND ACCELERATION ESTIMATION EMPLOYING NONUNIFORM SAMPLING

*L. Benner<sup>1,2</sup>, W. Wilkening<sup>1,2</sup>, H. Ermert<sup>1,2</sup>*

<sup>1</sup>Institute of High Frequency Engineering, Faculty of Electrical Engineering,  
Ruhr-Universitaet Bochum, Germany

<sup>2</sup>Ruhr Center of Excellence for Medical Engineering, Bochum, Germany

*Abstract* – Our group has previously proposed non-uniform sampling for flow velocity estimation. Standard Pulsed Wave Doppler (PWD) systems acquire an ensemble of  $N$  echoes per beam line at a constant pulse repetition frequency  $f_{\text{prf}}$ . The total time span determines the velocity resolution, and  $f_{\text{prf}}$  the unambiguous velocity range. The ensemble size  $N$  is by approximation inversely proportional to the frame rate, assuming that the system performs interleaving. If sampling intervals are chosen nonuniformly, the total time span can be increased, while keeping  $N$  and the shortest sampling interval constant. In this example, velocity range and frame rate are unchanged, and measurement accuracy for low flow velocities is gained at the expense of measurement accuracy for high flow velocities. The extended time span makes the flow estimation susceptible to effects of acceleration and decorrelation. Thus, we have refined the flow estimation algorithms by taking into account both effects.

### INTRODUCTION

Conventional PW Doppler systems acquire an ensemble of  $N$  echoes per beam at a constant repetition interval  $T_{\text{pri}} = 1/f_{\text{prf}}$ . Nonuniform sampling uses variable intervals lengths. The shortest interval defines the velocity range and longer intervals increase the total time span and, therefore, the velocity resolution without increasing  $N$ . (With interleaving, the frames rate is approximately reciprocal to  $N$ .) Thus, relative velocity resolution for low velocities is gained at the expense of relative velocity resolution at high velocities and SNR. This concept, which is known from RADAR [1, 2], has previously been adapted to medical ultrasound by our group, where cross correlation techniques are applied to all pairs of echoes (not only

to pairs of consecutive echoes) in the ensemble to determine scatterer displacement [3].

Two problems still had to be tackled: With increasing time span, acceleration becomes relevant, and it has to be considered to avoid ambiguity and incorrect velocity estimations. High flow velocities cause decorrelation. To measure slow axial flow velocities, it is important to exclude pairs of echoes that are decorrelated due to lateral or elevational flow.

### TIME SHIFT ESTIMATION

#### *Pulse Sequence*

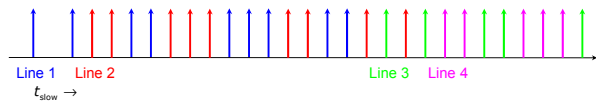


Fig. 1: The proposed sequence is interleaving compatible. Spaces longer than  $1 \cdot T_{\text{pri}}$  can be filled with acquisitions for other beam lines. Note that the sequences for line 2, 4 etc. are time-reversed.

The nonuniform pulse sequence discussed here is designed to have pulse intervals of different length distributed evenly over the total time span, where all length are multiples of the shortest interval  $T_{\text{pri}}$ . Furthermore, it is interleaving compatible, i.e. all intervals longer than  $T_{\text{pri}}$  can be used to acquire echoes for other beam lines.

#### *Modified Cross Correlations*

To estimate the flow velocity at a given depth  $z$ , all pairs of echo signals, i.e. not only pairs of consecutive echoes, are analyzed with respect to time shifts caused by moving scatterers. For a pair of echoes, the modified cross correlation functions (CCF, [3]) considers data within two sliding windows in either of the two echoes, where the windows are positioned symmetrically to the depth  $z$ . The time lag  $\tau$ ,

being the distance between the centers of the window in axial or fast time direction for which the CCF is maximal, is considered to be proportional to the axial displacement of scatterers. To avoid false maxima, which occur, if one window contains signals from a strong scatterer, the CCF values are normalized to the signal energies within the two windows.

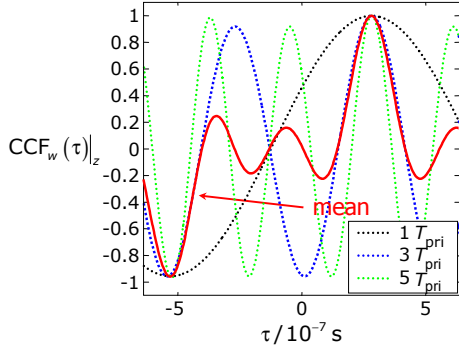


Fig. 2: Simulated CCFs, normalized to energies in sliding windows and rescaled so that the time lag  $\tau$  is proportional the velocity  $v$  independent of the time interval  $w \cdot T_{pri}$ . The CCF for the shortest time interval ( $1 \cdot T_{pri}$ ) exhibits only one maximum, i.e. it is aliasing-free. The CCFs for longer intervals show ambiguities, but the maxima are narrower, i.e. a better velocity resolution can be achieved. Taking the mean of the CCFs trades velocity resolution for unambiguity.

The CCFs will represent different time intervals. For a given velocity  $v$ , the displacement and, therefore, the time lag  $\tau$  is proportional to the time interval. We rescale the CCF to the time interval so that  $\tau$  is proportional to  $v$ . As can be seen in Fig. 2, long time intervals lead to narrower maxima, i.e. better velocity resolution, while shorter intervals have less or no ambiguities (fewer maxima).

#### VELOCITY AND ACCELERATION ESTIMATION

The CCFs (as illustrated in Fig. 2) represent a point on the slow time axis (see Fig. 1) that is defined by the center of the time interval. To account for acceleration, we arrange the CCFs along the slow time axis. The resulting diagram will be referred to as a V-T-diagram (V-T-D), see Fig. 3. A trajectory in this diagram describes the velocity as a function of slow time, where a horizontal line corresponds to a constant velocity. The task is to find a trajectory that fits the V-T-diagram best. In the following, different

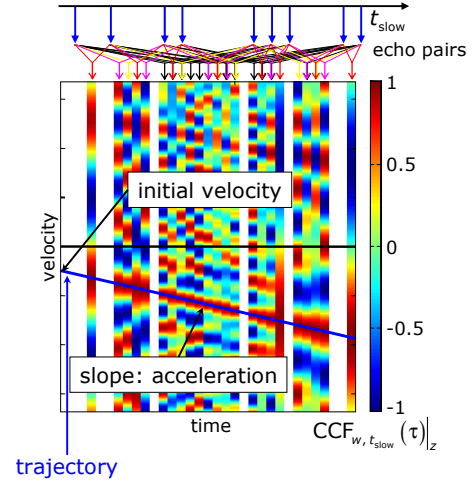


Fig. 3: V-T diagram showing cross correlation functions (see Fig. 2) along the slow time axis. Some pairs of echo signals may be centered on the same point of the slow time axis. In such cases, the functions are averaged. This diagram represents an in vivo measurement of the carotid artery.

strategies will be presented and analyzed. The strategies are limited to constant accelerations  $a$ .

#### Linear Regression through Maxima of V-T-D

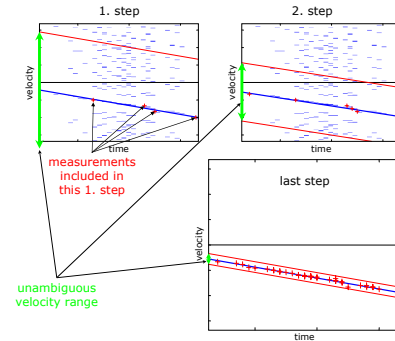


Fig. 4: In an iterative process, the initial flow estimate is determined by fitting a line through the maxima of the CCFs corresponding to time intervals of  $1 \cdot T_{pri}$ . The following steps include longer time intervals. Based on the previous estimates, the search range (red lines) is narrowed to exclude maxima that might be due to aliasing.

The first approach (Linear Regression through Maxima of V-T-D, LRM) is based on a V-T-D that shows only the maxima of the CCFs, see Fig. 4. The trajectory is determined in an iterative process: The first step considers the maxima belonging to the shortest time intervals ( $1 \cdot T_{pri}$ ). A linear regression through the maxima yields an initial, unambiguous

estimate for the trajectory. The next step additionally includes maxima for an interval length of  $2 \cdot T_{\text{pri}}$ . These CCFs will exhibit additional maxima that are due to aliasing (Fig. 2). To exclude those maxima, the search range is narrowed with increasing interval length (Fig. 4). The final iteration step includes all interval length. The iteration may also be terminated earlier, if the estimates do not change significantly from one step to the following or if the maxima of the following step are invalid because of decorrelation.

#### *Global Maximum Criterion*

A second approach is to determine the trajectory along which the sum of CCF values is maximal. The trajectory in Fig. 3 fulfills this requirement. It is obvious, however, that the aforementioned sum as a function of velocity and acceleration will be characterized by many local maxima. Thus, the full range of velocities and accelerations is searched in a small-enough grid, which is determined by the longest time interval. Once the global maximum is found in the resolution of the search grid, the estimate can be refined using gradient-based methods.

#### *Symmetry Criterion*

Fig. 3 reveals that the CCFs are symmetrical to the likeliest (correct) trajectory. Based on this observation, a third estimator was developed. The optimization criterion is the symmetry of the cross correlation values to a given trajectory. The search method is the same as for the Global Maximum approach.

### DECORRELATION AND CONFIDENCE

We have to differentiate between two sources of decorrelation: One source is given by e.g. motion artifacts, noise, or other kinds of interference. Another source is related to the flow. Elevational and lateral flow components cause decorrelation. Even if flow is purely axial, displacement estimations may not be reliable, unless the displacement is small enough. We, therefore, limit the search range for axial displacements to  $\pm\lambda/4$ . Furthermore, maxima can be excluded (LRM method), if the CCF values are below some threshold, e.g. 0.5.

In addition to velocity and acceleration, a confidence parameter is computed. For all estimation approaches, it is given by the sum of the CCF values along the estimated trajectory, where all values are excluded that are below a certain threshold (0.5) or

definitely due to aliasing according to the estimated velocity and the length of the time interval. This confidence value turned out to be a reliable marker of flow.

### WALL FILTERS

The goal is to eventually implement an adaptive wall filter. In a first step, the processing will be performed on the original data. Thus, the algorithm will determine the velocity of tissue. Based on the spatial distribution of velocities and echo amplitudes, artifacts will be eliminated. Then, the data will be realigned so that signals from tissue are stationary. By subtracting the mean value in slow time direction from all samples at a given depth, stationary signals are eliminated. In the next step, the blood flow velocities can be estimated.

This approach is extremely time consuming. The in vivo data presented here was processed by locally subtracting the mean in slow time direction.

### DATA ACQUISITION

Data was acquired using a Siemens Sonoline<sup>®</sup> Antares System equipped with a VF10-5 transducer (linear array, width: 4 cm, center frequency: 7.5 MHz). 18 echoes were acquired per beam line at  $f_{\text{prf}} = 6.25 \text{ kHz}$ . 9 of the echoes were taken out of the echoes representing the proposed pulse sequence. A human carotid artery was imaged over several heart cycles so that different flow scenes could be analyzed. RF data was acquired with 16 bits resolution at 40 MHz sampling rate using the Axius Direct Ultrasound Research Interface.

### RESULTS

The RF data was analyzed applying the three different algorithms described above. The LMR algorithm is the fastest, while the Symmetry Criterion, being the slowest, turned out to be most robust with respect to noise and clutter robustness. Fig. 5 shows in vivo images under low flow and high flow conditions. Note that the decision to overwrite the B-mode image with flow data is solely based on the confidence parameter. Also note that the color map represents different velocity ranges underlining the ability of nonuniform sampling approaches to handle wide velocity ranges.

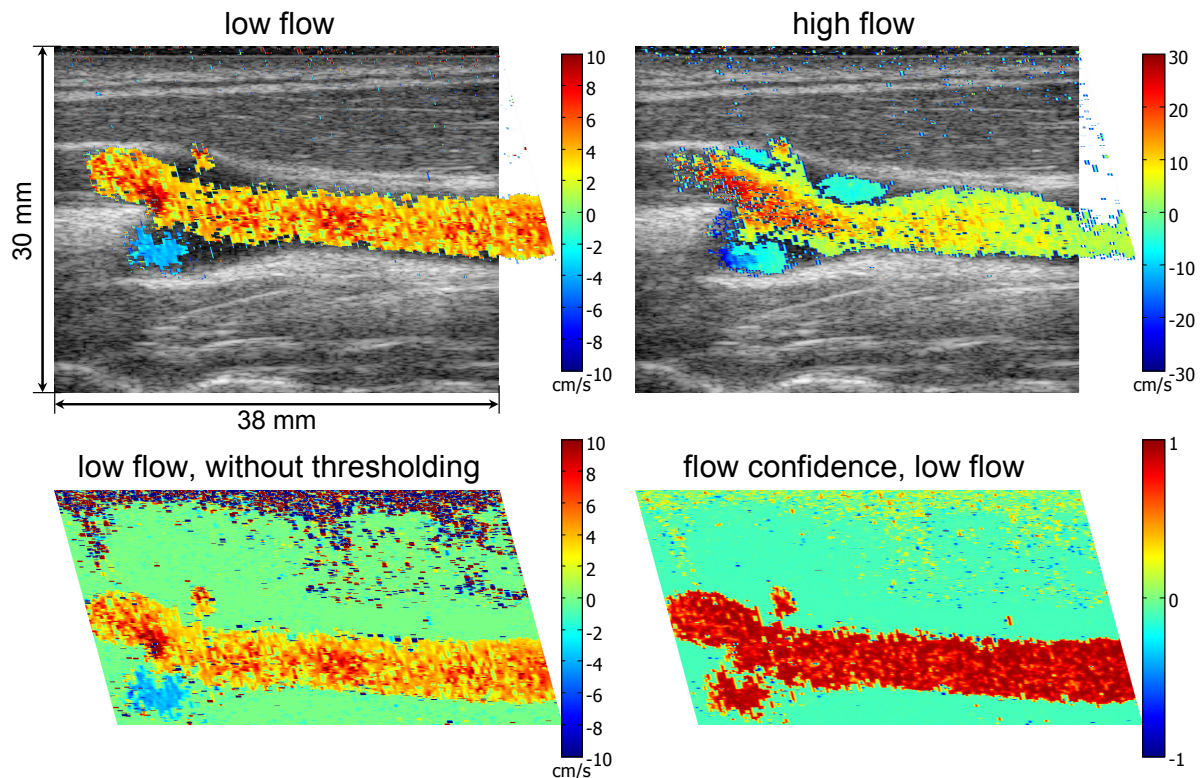


Fig. 5: With only 9 echoes per beam line, the proposed nonuniform sampling approach provides satisfactory velocity resolution for low and high flow at  $f_{\text{prf}} = 6.25 \text{ kHz}$ . The flow image without thresholding illustrates that the symmetry criterion even correctly estimates the tissue flow from the residual signal after wall filtering. The mean of CCF values along the estimated trajectory, where decorrelated or aliased measurements are excluded, serves as a confidence criterion for flow. This parameter is exclusively used for thresholding rather than the intensity of the underlying B-mode image or a velocity threshold.

## CONCLUSIONS

By taking into account acceleration and decorrelation, the reliability of nonuniform sampling approaches for flow imaging was improved significantly compared to the initial results presented in [3]. The newly developed algorithms yielded similar results, where the slowest algorithm (Symmetry Criterion) is least sensitive to noise and artifacts.

Adaptive wall filters have yet to be sped up to be usable. Eventually, real nonuniform sequences have to be implemented, since reverberation may create artifacts that cannot be noticed, if the nonuniform sequence is extracted from a uniform sequence.

## ACKNOWLEDGEMENT

We thank Siemens Medical Systems, Inc., Ultrasound Group for their assistance with the Axius Di-

rect Ultrasound Research Interface.

The work was carried out by the Ruhr Center of Excellence for Medical Engineering (KMR Bochum), BMBF (Federal Ministry of Education and Research, Germany) grant 13N8017.

## REFERENCES

- [1] E. S. Choroboay, M.E. Weber, "Variable-PRI processing for meteorologic Doppler radars," Proceedings of the 1994 IEEE National Radar Conference (1994), pp. 85-90.
- [2] Z. Banjanin, D.S. Zrnić, "Clutter rejection for Doppler weather radars which use staggered pulses," IEEE Transactions on Geoscience and Remote Sensing, vol. 29(4), pp. 610-620, 1991.
- [3] Wilkening W, Brendel B, Ermert H. Fast, extended velocity range flow imaging based on nonuniform sampling using adaptive wall filtering and cross correlation. Proceedings of the IEEE Ultrasonics Symposium, 2002, 2B-3.